Turkish Journal of Civil Engineering, 2025, xxxx-xxxx, Paper xxx, ***Research Article***

Optimization of Mechanical Properties of Mixed Fiber Concrete by Taguchi Method: Impact, Compressive and Flexural Strength

Mehmet Hanifi ALKAYIŞ[1*]
Celalettin BAŞYIĞIT[2]

ABSTRACT

This study investigates the mechanical properties of fiber-reinforced concrete by evaluating the effects of steel, polypropylene and basalt fibers on the compressive, flexural and impact strength of concrete. Experimental studies and optimization were carried out by determining the concrete mixture by creating Taguchi L16 (4^4) matrix. As a result of the analysis, steel fibers significantly increased the mechanical and impact strength of concrete due to their high strength and hooked end structures. On the other hand, the effect of polypropylene and basalt fibers was more limited. Basalt fibers, especially due to their microstructure and polypropylene fibers, had limited effectiveness due to their lower tensile strength. The amount of binder also plays an important role in the overall strength of concrete and it was found that the optimum binder content increased the strength of concrete. The results obtained from Taguchi analyses provide an important roadmap for the advancement of concrete technology. It is important to understand the effects of different types and amounts of fibers on the mechanical and impact properties of concrete.

Keywords: Fiber reinforced concrete, impact resistance, mechanical properties, taguchi optimization.

1. INTRODUCTION

With increasing human needs, the construction sector is producing a variety of structures for different purposes, employing numerous building materials. Concrete, the most widely used material, has been extensively studied for its mechanical properties like compressive, tensile, and flexural strength, and more recently, its impact resistance. Various methods have been

---

Note:
- This paper was received on July 31, 2024 and accepted for publication by the Editorial Board on April 8, 2025.
- Discussions on this paper will be accepted by xxxxxxx xx, xxxx.

- https://doi.org/

1 Süleyman Demirel University, Department of Civil Engineering, Isparta, Türkiye
mehmethanifialkayis@gmail.com - https://orcid.org/0000-0003-0177-043X

2 Süleyman Demirel University, Department of Civil Engineering, Isparta, Türkiye
celalettinbasyigit@sdu.edu.tr - https://orcid.org/0000-0003-0084-1320

* Corresponding author

developed to assess concrete's impact resistance based on the type of loading and the feasibility of the experiment [1].

The impact resistance of a concrete element directly relates to its energy absorption capacity and toughness. For high toughness, indicated by the area under the stress-strain curve, the material must be ductile and possess high strength. Despite concrete's inherent brittleness in standard designs, efforts are ongoing to enhance its ductility and strength [2].

While traditional concrete has low impact resistance, its composite nature allows for potential improvements. However, the multiple components of concrete significantly affect its mechanical properties, including impact resistance. Concrete components include aggregate mineralogy and physical properties, water-cement ratio, and additives such as type, amount, and physical/mechanical properties. Experimental conditions, such as concrete temperature and loading rate, also influence concrete's impact resistance, as depicted visually in Fig.1 [3].

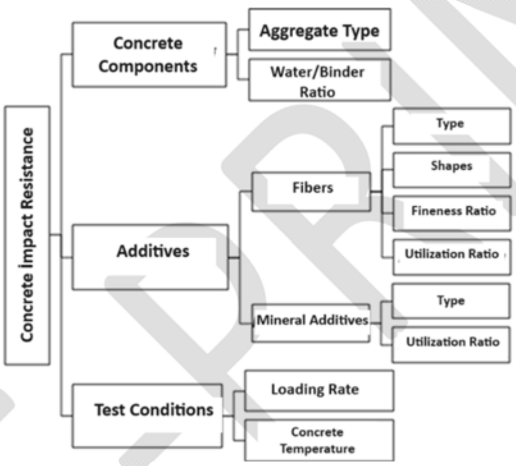

Figure 1 - Factors influencing concrete impact resistance [3]

Fiber-reinforced concretes' impact resistance has been investigated in terms of the effect of aggregate maximum particle size, one of the main parameters of concrete. Uniaxial compressive strength, split tensile strength, ultrasonic testing, and the impact test recommended by ACI Committee 544 were conducted. From the experimental results, it is recommended that the aggregate maximum particle size should not exceed 20 mm for impact resistance [4].

One of the key parameters affecting concrete strength and durability is the water-cement ratio. Research indicates that decreasing the water-cement ratio increases concrete strength and consequently enhances impact resistance [5]. However, some studies suggest that concrete with a higher void ratio due to a lower water-cement ratio exhibits higher impact resistance [6]. Therefore, the influence of the water-cement ratio on impact resistance relative to compressive strength remains a topic open to further research.

Mineral additives are another factor that enhances concrete strength. Particularly, additions like silica fume, blast furnace slag, fly ash, metakaolin, etc., can improve concrete strength and durability, thereby increasing impact resistance. Studies have shown that the addition of silica fume improves fiber distribution and further enhances strengths, especially in fiber-reinforced specimens [7].

One of the most important parameters affecting concrete impact resistance is the type and amount of fiber. Various types of fibers can be added to concrete, including steel, polypropylene, glass, basalt, polyamide, polyvinyl alcohol, ceramic, polyethylene, nylon, Kevlar, and natural fibers. Among these, steel and polypropylene fibers are the most commonly used, with steel fibers being particularly effective for improving impact resistance. These fibers not only enhance the mechanical properties of concrete but also provide tailored solutions for specific challenges, such as dynamic loads and extreme environmental conditions. [3]. It has been determined that high ductility steel fibers with hooked and crimped ends positively impact impact resistance. Furthermore, increasing fiber fineness and usage rate also contributes to enhanced impact resistance [8].

According to ACI 544 standards for steel fiber-reinforced concrete, the fiber volume fraction should be between 0.5% and 1.5%. Exceeding this level reduces concrete workability and may lead to segregation. However, special fiber addition and placement techniques can increase the fiber percentage. Moreover, in high-strength concretes with compressive strength exceeding 40 MPa, the addition of short fibers at a rate of 2% can increase ductility [9,10].

In terms of shape, spiral and hooked-end steel fibers exhibit better performance under impact load compared to other types of steel fibers. Hooked-end steel fibers reduce crack width, spacing, and damage mechanisms under low-speed impact [10]. Additionally, macro fibers have been observed to provide more beneficial results in impact resistance compared to microfibers. It is also emphasized that a suitable combination of macro and micro steel fibers yields the most effective results [11]. Micro fibers, due to their size, create a denser fiber distribution within the matrix, preventing cracks from reaching the macro level and improving behavior in the elastic region. Macro fibers, on the other hand, enhance the modulus of elasticity, tensile, and flexural strengths, control macro-level cracks, and improve post-peak behavior [12].

Today, there is a need for promising optimization methods to determine the best concrete mix with minimal testing. One of the most popular optimization methods is the design of Taguchi experiments. The Taguchi method aims to minimize the variance of responses close to the optimal response by finding optimal levels for control factors [13].

Tanyıldızı and Şahin [14], examined the effects of control factors such as silica fume percentage, temperature, and polymerization type on polymer-modified concrete. They used an L32 orthogonal array to conduct their experiments. Variance analysis (ANOVA) identified silica fume as the most effective factor.

Sharifi et al. [13] used the Taguchi optimization method to model the optimum mix design of high-strength self-compacting concrete. They designed a Taguchi L18 matrix based on parameters such as cement content, water/cement ratio, and mixing time, which are the most important parameters affecting concrete mix design. Variance analysis was also used to evaluate effective factors and optimal mix design. Mehta et al. [15] used the Taguchi method to examine the factors affecting the compressive strength of geopolymers. ANOVA was used to examine the effects of factors on compressive strength, and signal-to-noise ratio graphs were used to obtain the most suitable design.

The studies reviewed have shown that fiber content, fiber type, and properties (length, aspect ratio, fiber type) primarily affect compressive, flexural, and impact strengths. However, how this effect manifests in hybrid fiber-reinforced concretes and which parameter most affects impact resistance has been investigated through Taguchi methods and ANOVA analyses. An experimental study program was designed using an orthogonal array L16(4^4) that includes all factors and levels to determine the optimal mix according to the highest-best criterion based on the Taguchi method. The experimental results were analyzed according to the Taguchi method and ANOVA to confirm the hypothesis.

2. MATERIALS AND METHOD

2.1. Materials and Mix Design

In this study, cement, silica fume, macro fibers (steel and polypropylene), microfibers (basalt), coarse aggregate (dolomite and limestone), fine aggregate (dolomite), water, and superplasticizer were used for the experimental series. The materials used and their properties are described below under headings.

CEM II/A-M (P-LL) 42.5 R class Portland Composite cement obtained from Isparta Göltaş Cement Co. was used in the experiments. CEM II 42.5 A-M (P-LL) cement is produced by grinding Portland cement clinker with a defined amount (12-20%) of pozzolan additive, setting regulator gypsum, and minor additional component (limestone) according to standards. The pozzolan additive (blast furnace slag) used during production enhances the workability of concrete and mortar, facilitating the casting of dense mass concrete. This type of cement was chosen due to its fiber addition and low water-to-cement ratio, despite its low workability. The chemical properties of this cement are provided in Tables 1 and 2.

Table 1 - Chemical properties of the cement

Component	***Rate (%)***
Blast furnace slag	*12-20*
SiO_2	*15-19*
Al_2O_3	*3.7-6*
Fe_2O_3	*2.65-4.90*
CaO	*58-66*
MgO	*1-3.50*
SO_3	*<4*
Na_2O	*0.002-0.32*
Cl^-	*<0.10*
Loss on Ignition (LOI)	*3.80-12*

Table 2 - Physical properties of the cement

Physical Property	***Amount***
Fineness (%)	6.81
Specific gravity (g/cm^3)	3.01
Specific surface area (cm^2/g)	4403
Initial setting (hours-minutes)	2h-56m
Final setting (hours-minutes)	3h- 24m
Volume expansion (mm)	0.50
2-day compressive strength (MPa)	27.46
20-day compressive strength (MPa)	51.03
Water requirement (%)	29.00

Due to its high fineness and spherical shape, which provide good cohesion and resistance to segregation, silica fume has been chosen as a mineral additive material compliant with ASTMC-1240 standard. Table 3 presents the properties of the silica fume used in the experiments.

Table 3 - Technical specifications and standards for silica fume

Properties	***Amount***	**ASTM C-1240**
SiO_2 (%)	96.1	min 93
H_2O (%)	0.19	max 0.3
+45 micron up (%)	0.58	max 2.5
Bulk density (kg/dm^3)	0.55-0.65	-
Loss of glow	1.81	L.O.I. max 3.5

In this study, basalt fibers were chosen to mitigate micro-cracking in the concrete, while steel and polypropylene fibers were selected to enhance the ductility, toughness, and impact resistance of hardened concrete. Two hooked-end steel fibers, 6 cm in length, conforming to ASTM A820 standard, and polypropylene fibers, 5 cm in length, conforming to ASTM CIII6 CE standard, as well as 12 mm long basalt fibers, were used in the study. Images of these fibers are provided in Figure 2.

In accordance with relevant standards and regulations, fiber lengths were chosen as 6 cm for macro fibers to mitigate larger cracks between aggregates, and 12 mm for microfibers to address finer cracks at aggregate interfaces. Leveraging the high elasticity modulus and rigidity of steel and polypropylene fibers aims to control cracking due to impact loads. The combined use of polypropylene and steel fibers can improve the performance of concrete. While polypropylene fibers contribute to the prevention of microcracks and increased workability, steel fibers are effective on macrocracks and provide high impact resistance. In addition, PPL of a different length (54 mm) than steel fibers was used to create physical synergy. To minimize potential debonding issues in fiber-concrete adhesion, a combination of steel, polypropylene, and basalt fibers was preferred. Steel, polypropylene, and basalt fibers are combined in fiber-concrete composites to improve adhesion and reduce debonding. Steel fibers enhance tensile strength, impact resistance, and crack control, while polypropylene fibers reduce early-age cracking and shrinkage, and help prevent debonding due to their low surface energy. Basalt fibers offer excellent thermal stability, corrosion resistance, and improved bonding strength, enhancing the durability of the composite [16]. The synergy of these fibers provides a stronger, more durable concrete, improving its performance under dynamic loads and harsh environments by combining the unique physical and mechanical properties of each fiber type.The random distribution of fibers within concrete aims not only to bridge cracks but also to introduce an innovative approach leveraging the properties of three different types of fibers.

Figure 2 - The fibers used in concrete; a) steel fiber, b) polypropylene fiber, c) basalt fiber.

Macromesh54 Polypropylene Fiber (PF) produced by Atlas company was used (Figure 3). The addition rate of polypropylene macro fibers to concrete is recommended between 1.5-9 kg/m³ depending on the targeted engineering properties. Macromesh 54 reduces segregation and maintains aggregate-cement integrity, enhancing cohesion and preserving concrete integrity. Compared to steel alternatives, it is lighter, corrosion-resistant, and economically advantageous. It enhances surface wear resistance, contributing to sustainable surfaces. Basalt fibers are widely used for various purposes in constructions, enhancing impact resistance in concrete, and increasing resistance to water, chemicals, freezing, fire, and improving durability. Here, 12 mm long basalt fibers were used in concrete manufacturing. The properties of the fibers used are provided in Table 4.

Crushed stone, due to its rougher surface texture compared to gravel, is predominantly used as aggregate in high-strength concrete for its superior matrix-aggregate bond and thereby enhanced strength [17]. Additionally, crushed stone has a higher surface area to volume ratio than rounded gravel. To increase total bond contribution, the maximum aggregate size is typically kept below 19 mm, necessitating an increase in paste content to ensure adequate workability. The combination of a low water-to-cement ratio and small maximum aggregate size implies a high cement content, generally ranging from 400 to 600 kg/m^3 [18].

Table 4 - Physical and mechanical properties of fibers

Feature	***Steel Fiber***	***Polypropylene Fiber***	***Basalt Fiber***
Length (mm)	*60*	*54*	*12*
Diameter (mm)	*0.90*	*0.1*	*<0.02*
Aspect Ratio (l/d)	*65*	*540*	*680*
Melting Point (°C)	*1500*	*170*	*1450*
Slenderness	*65*	*-*	*>600*
Density (t/m^3)	*7.85*	*0,91*	*2.65*
Tensile Strength (MPa)	*1500*	*750*	*4840*
Modulus of Elasticity (GPa)	*210*	*5.75*	*89*
Fiber amount (Piece/kg)	*3200*	*200000*	-

High-strength concrete has undergone significant development based on the type and proportions of cement, mineral additives, superplasticizer types, and the mineralogical composition of coarse aggregates.

In this study, natural crushed stone of dolomitic limestone origin from Isparta Altınkök aggregate quarry was used. Crushed and screened aggregates of 0-4 mm and 4-11 mm were utilized as sand and gravel aggregates in the crushing and screening facilities (Figure 3). The technical specifications of dolomitic limestone aggregates (DKA) are provided in Table 5. Considering the particle distribution of natural crushed stone aggregates, aggregate sizes ranging from 4-12 mm were selected at 15% each, and 0-4 mm at 70%, to prepare a mixture aggregate in accordance with TS802 gradation standards.

Figure 3 - Aggregates used in concrete; a) fine aggregate (0-4 mm), b) coarse aggregate (4-11.2 mm).

Table 5 - Physical properties of the aggregate

Properties	***Fine Aggregate***	***Coarse Aggregate***
Grain Size (mm)	*0-4*	*4-11.2*
Specific weight	*2.69*	*2.77*
Water absorption rate (%)	*3.30*	*1.70*
Mixing proportions (%)	*70*	*30*

Superplasticizer additives are used to achieve the desired workability of concrete production with low water/cement ratio. They not only increase the strength of concrete but also facilitate its workability and pumping to desired locations and heights. Typically categorized by their chemical origins, lignosulfonate-based additives are referred to as normal, melamine and naphthalene sulfonate formaldehyde-based ones as superplasticizers, and polycarboxylate-based ones as hyperplasticizers. Lignosulfonate-based additives exhibit both plasticizing and air-entraining effects. Concretes produced with these additives not only exhibit high compressive strength but also high resistance to freeze-thaw cycles. In this study, superplasticizer was used at a rate of 1.5-2% due to the production of concretes with 3 types of fibers. Technical specifications of the superplasticizer are provided in Table 6. Additionally, tap water from the municipal supply of Isparta city was used as mixing water and curing water in concrete production.

Table 6 - Technical specifications of super plasticizer

Properties	***Value***
Chemical content	*Melamin Sülfonat*
Colour	*Brown Liquid*
pH	*6-9*
Density (g/cm3)	*1.05*
Chlorine content (%)	*<10*
Alkali content (%)	*ASTM C 494 Tip F*
Standard	*%1-2*
Consumption	*Melamin Sülfonat*

2.2. Design Specifications and Production of Prefabricated Concrete Elements

In the scope of the experimental study program, a total of 16 concrete mix designs were developed using the Taguchi method, which includes an orthogonal array L16(4^4) showing all factors and levels. In all series, the water-cement ratio (w/c ratio) was maintained at 0.38. However, with the addition of SP, the water/binder ratio became 0.40. Additionally, a superplasticizer was used at a 2% dosage rate. The total air content was set at 2% according to TS802. Binder dosage was varied at four levels based on literature: 400, 450, 500, and

550 units. The steel fiber content was varied volumetrically as a percentage of the total concrete volume at 0%, 0.5%, 1%, and 1.5%. The polypropylene fiber content was adjusted at 0%, 0.15%, 0.3%, and 0.45%, and the basalt fiber content was adjusted at 0%, 0.025%, 0.05%, and 0.075%. Furthermore, 10% of the cement was substituted with silica fume across all mixtures.

The impact tests in the literature were conducted on concrete series with basalt fiber (BF) content ranging from 0.05% to 0.1% of the concrete volume, and macro synthetic polypropylene fiber (PPF) content ranging from 0.15%, 0.25%, 0.35%, to 0.5% of the concrete volume. The test results showed that both BF and PPF fibers could increase the impact resistance of concrete, but the optimum hybrid fiber mixture was the 0.075%-0.35% (BF-PPF) sample, which exhibited the best impact resistance [19]. Additionally, the maximum polypropylene fiber (PPF) content is limited to 0.45% due to the design constraint that the total fiber content should not exceed 2% of the concrete volume.

The aggregate amount used was calculated by subtracting the volumes of cement, silica fume, water, fibers, and air from the total volume. These levels were incorporated into the matrix, resulting in the concrete series as shown in Table 7.

Table 7 - Amounts of materials used for 1 m^3 concrete according to Taguchi L16 matrix (kg)

Series	*SF*	*Cement*	*SF*	*PPF*	*BF*	*0-4 mm Agregate*	*4-11.2 mm Agregate*	*SP*	*Water*	*w/b*
K1	40	360	0	0	0	1294.62	554.84	8	152	0.40
K2	40	360	39	1.37	0.68	1292.22	553.81	8	152	0.40
K3	40	360	78	2.73	1.35	1289.83	552.78	8	152	0.40
K4	40	360	117	4.1	2.03	1287.44	551.76	8	152	0.40
K5	45	405	0	1.37	1.35	1226.10	525.47	9	171	0.40
K6	45	405	39	0	2.03	1225.68	525.29	9	171	0.40
K7	45	405	78	4.1	0	1226.92	525.82	9	171	0.40
K8	45	405	117	2.73	0.68	1226.49	525.64	9	171	0.40
K9	50	450	0	2.73	2.03	1158.99	496.71	10	190	0.40
K10	50	450	39	4.1	1.35	1159.40	496.88	10	190	0.40
K11	50	450	78	0	0.68	1163.74	498.74	10	190	0.40
K12	50	450	117	1.37	0	1164.14	498.92	10	190	0.40
K13	55	495	0	4.1	0.68	1096.07	469.75	11	209	0.40
K14	55	495	39	2.73	0	1098.45	470.76	11	209	0.40
K15	55	495	78	1.37	2.03	1095.22	234.69	11	209	0.40
K16	55	495	117	0	1.35	1097.60	235.20	11	209	0.40

2.3. The Production and Compaction of Concrete Series

The process of producing fiber-reinforced concrete samples is given in Figure 4.

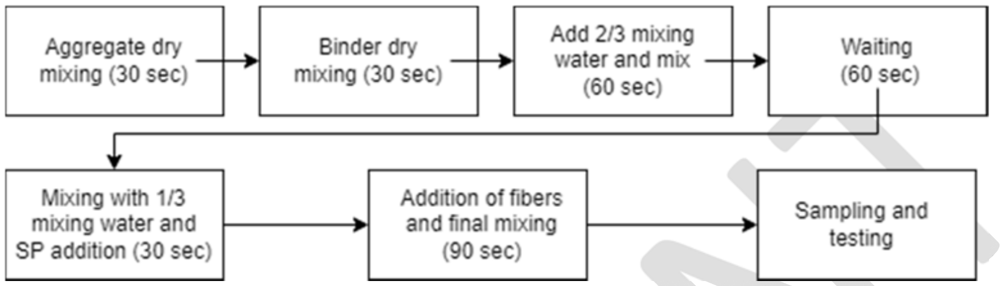

Figure 4 - Concrete mixing and production stages

Figure 5 - Concrete Production: a) fibers used, b) dry mixing, c) addition of liquid and mixing, d) compaction and finishing

In the production of fiber-reinforced concrete, aggregates were first emptied into the mixer from largest to smallest size and mixed. Cement and mineral additives (with a water-to-cementitious materials ratio of 0.40) were added dry to the mixer and blended into the concrete mix (Figure 5b). After mixing with a portion of the mixing water and chemical admixture, the remaining mixing water was added to the rotating mixer and blended. The mixer was then stopped. Diluted chemical admixture was poured into the mixer during the mixing process and blended. Fibers were slowly sprinkled in from smallest to largest size according to the size of the fibers. The fibers were carefully mixed until they were evenly distributed throughout the fresh concrete mix. A photograph of the fiber-reinforced fresh concrete mix after mixing is shown in Figure 5.

The produced concretes were cast into molds of various sizes for each experiment, compacted using a vibrating table, and then settled. Unit volume weight, Slump, and Walz slump test results for the concretes are shown in Figure 6 and the measurement values are presented in Table 8. The determination of compactability degree involves assessing the consistency of fresh concrete and its ability to be fully compacted. The test is suitable for concretes with a specified compactability degree (c) ranging from 1.04 to 1.46, particularly recommended for concretes with Slump values below 4 cm [20].

Table 8 - The density and slump values of the experimental series

Series	***Unit volume weight (t/m^3)***	***Slump (cm)***	***Walz degree of compression***
K1	*2.44*	*6.00*	*1.11*
K2	*2.45*	*2.50*	*1.19*
K3	*2.47*	*2.00*	*1.29*
K4	*2.52*	*1.00*	*1.40*
K5	*2.48*	*1.90*	*1.36*
K6	*2.61*	*1.60*	*1.38*
K7	*2.60*	*1.70*	*1.38*
K8	*2.58*	*0.50*	*1.46*
K9	*2.49*	*3.00*	*1.25*
K10	*2.51*	*2.00*	*1.30*
K11	*2.55*	*2.00*	*1.33*
K12	*2.58*	*1.00*	*1.41*
K13	*2.46*	*3.00*	*1.20*
K14	*2.52*	*2.00*	*1.26*
K15	*2.53*	*1.50*	*1.28*
K16	*2.57*	*1.00*	*1.39*

The initial sample size was found to be inappropriate for the study due to the wall effect (100 cube). However, the sample size was subsequently revised to a larger dimension (150 mm cube) to ensure more uniform fiber distribution and more reliable test results. In addition, since there is no limitation in the literature regarding the use of prism samples, casting was made in 100x100x500 dimensions. In addition to the slump test, the Waltz test was also conducted at this stage (see Figure 6).

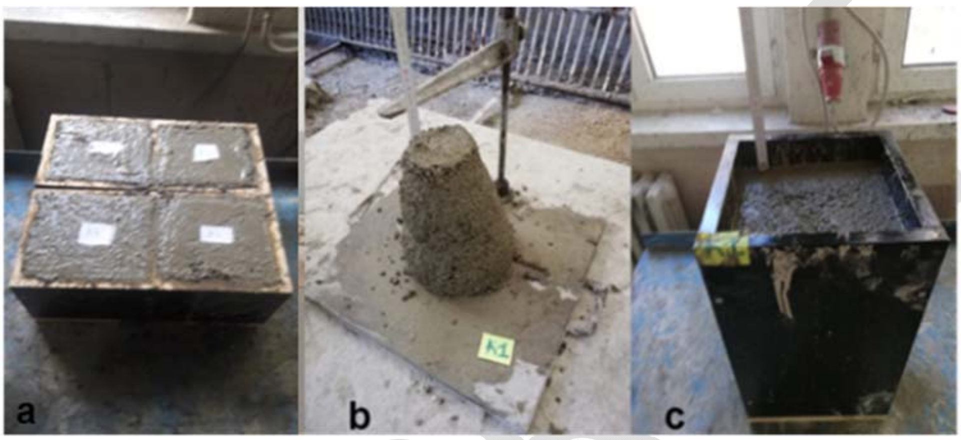

Figure 6 - Fresh Concrete Tests: a) Unit volume weight determination, b) Slump test, c) Walz test

The concrete specimens, placed in molds, were demolded approximately 24 hours later and then cured in a lime-saturated curing tank at a temperature of 20±2°C for 28 days, followed by further laboratory curing up to 90 days. The sample sizes and numbers for each experimental series are provided in Table 9.

Table 9 - The sample sizes and quantities produced for the experimental series.

Test	**Sample shape**	**Dimensions (mm)**	**Number of samples in each series**
Compressive strength	Cube	*150x150x150*	*9*
Bending strength	Beam	*100x100x500*	*3*
Impact resistance	Beam	*100x100x500*	*3*

2.4. Hardened Test Results of the Concrete Series.

Compression tests were conducted on cube specimens produced according to TS EN 12390-3 standards. The compression tests on cube specimens were carried out using a loading machine with a capacity of 200 tons, applying a loading rate of 0.3 to 0.5 N/mm²/s. The compressive strength results at 7, 28, and 90 days for each series are presented in Table 10.

Table 10 - Compressive strength values (MPa) of the experimental series

Series	***7 Days***	***28 Days***	***90 Days***
K1	20.10	31.36	34.05
K2	17.57	27.75	34.77
K3	21.24	33.58	38.07
K4	24.65	39.73	38.66
K5	23.23	33.41	42.13
K6	27.98	34.43	48.34
K7	29.71	40.12	51.75
K8	27.07	37.20	50.66
K9	31.91	40.69	48.77
K10	28.92	44.43	50.71
K11	34.77	42.36	52.69
K12	35.46	48.63	57.78
K13	24.58	40.92	45.41
K14	32.46	44.23	51.55
K15	38.21	48.32	55.37
K16	33.23	53.35	60.02

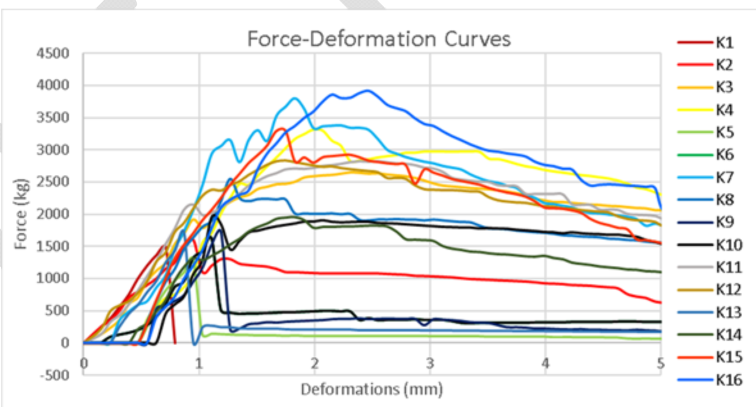

Figure 7 - Load-deflection curves of the concrete series

Typically, the 28-day compressive strength is considered the standard for assessing concrete's final strength, as it is believed to represent the material's maturity. However, the 7 and 90-

day strengths have been included to provide a broader perspective on the concrete's early and later strength development, they were not directly analyzed in relation to other factors.

The flexural strength test was conducted on 28-day, 100 mm x 100 mm x 500 mm prismatic (without notches) specimens produced according to standards, and the test results are provided in Table 11. Additionally, in beam specimens, the bending test continued until a deflection of 5 mm was achieved at the midspan of the beam, and the load-deflection values were recorded using a data acquisition system (see Figure 7). Table 11 also includes the flexural strength and energy absorption capacities (EAC).

The drop hammer impact test was conducted based on modified recommendations from ACI Committee 544, where impacts were repeatedly dropped on the same point of the test specimen. In this modified impact test, a 4.54 kg mass drop hammer, released from a height of 0.5 m above the top of the specimen as shown in Figure 8, generated an impact energy of approximately 22.25 J at a velocity of 3.13 m/s. The clear span of the specimen is 300 mm.

Table 11 - Flexural strength and EAC values of the experimental series

Series	***Flexural Strength (MPa)***	***EAC (kg.mm)***
K1	5.04	464.89
K2	6.07	5027.34
K3	9.82	11144.19
K4	10.90	12057.65
K5	5.15	921.97
K6	6.09	2663.08
K7	10.36	11072.98
K8	10.74	9342.41
K9	5.67	1756.76
K10	6.49	7318.81
K11	11.03	11422.01
K12	11.66	12475.28
K13	6.51	1470.11
K14	7.27	7179.30
K15	11.94	12325.08
K16	13.84	14632.99

The number of blows required to initiate the first visible crack, Ni, and the final failure, Nf, were recorded and utilized to determine the initial crack and ultimate impact energy of the concrete as follows:

$E_{impact}=N*g*m*h*0.9$ (1)

E_{impact} is the impact energy in joules (J), N is the number of impacts, g is the acceleration due to gravity (approximately 9.81 m/sn^2), m is the mass of the hammer (4.54 kg), h is the height from which the hammer is dropped (500 mm). The coefficient 0.90 accounts for factors such as efficiency or energy losses during impact.

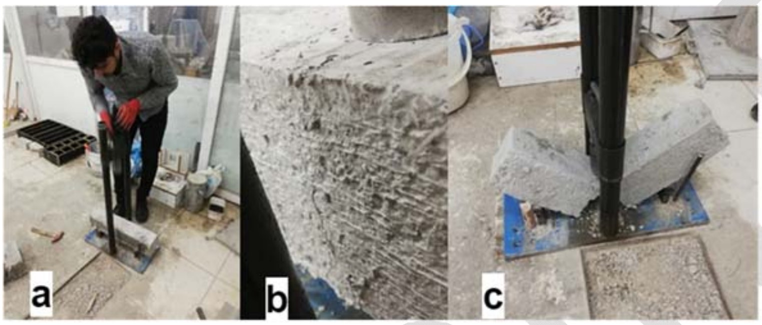

Figure 8 - Concrete impact test: a) dropping of the weight, b) initiation of the first crack, c) ultimate failure

Table 12 - First and fracture impact count and energy values of the experimental series

Series	*Number of first crack blows*	*Number of breaking blows*	*First Crack energy (Joules)*	*Fracture energy (Joules)*
K1	1.00	1.00	20.04	20.04
K2	1.67	19.00	33.40	380.79
K3	3.00	33.50	60.13	671.40
K4	4.00	43.00	80.17	861.80
K5	1.00	1.67	20.04	33.40
K6	1.67	14.00	33.40	280.59
K7	3.67	40.00	80.17	851.78
K8	4.33	40.33	86.85	808.35
K9	1.33	2.33	26.72	46.76
K10	2.67	26.33	53.44	527.77
K11	3.00	36.00	60.13	721.51
K12	4.33	62.67	86.85	1255.95
K13	1.67	2.67	33.40	53.44
K14	2.00	22.67	40.08	454.28
K15	3.33	42.00	66.81	841.76
K16	5.00	65.00	100.21	1302.72

The impact energy is adjusted by a factor of 0.9 due to the hammer moving back and forth between the rails. The number of impacts until the first crack and failure of the specimens, along with the calculated impact energies, are presented in Table 12.

3. EXPERIMENTAL RESULTS: TAGUCHI OPTIMIZATION AND ANOVA ANALYSIS

Before conducting the experiment, it is essential to design the experiment in a way that will provide the maximum information when investigating the real difference among effects for the problem to be solved. The reliability of the decision to be made depends on determining an appropriate experimental strategy. In a Full Factorial Design (FFD), equal numbers of observations are made for each level of each factor to determine the independent effects of factors on product performance. This feature is called orthogonality. This experimental strategy encompasses the other described experimental strategies, and it allows observing the variability's effect on performance when one factor level is kept constant and the levels of other factors are varied.

When conducting a Full Factorial Design (FFD) is not economical, easy, or feasible, a Fractional (Partial) Factorial Design, which involves fewer experiments, is used. The Taguchi method applied in the study is a type of fractional factorial design. Although the number of experiments would be 256 in a Full Factorial Design, it has been reduced to 16 using the Taguchi Method.

In Taguchi Experimental Design, the obtained experimental results are evaluated by converting them into Signal-to-Noise (S/N) ratios. Taguchi developed a series of statistics called signal-to-noise ratios to be used as performance criteria in experimental design with the aim of reducing variation. Depending on the nature of the objective, Taguchi divided it into three types and defined a different signal-to-noise ratio for each [21].

Smallest - Best

In this type of problem, the target value for the quality variable is zero. In this case, the signal-to-noise ratio is defined as follows:

$$\frac{S}{N} = -10 * \log_{10}\left[\frac{1}{n}\left(\sum_{i=1}^{n} {y_i}^2\right)\right] \tag{2}$$

Largest – Best

Here, the target value is infinite, and the signal-to-noise ratio is defined as:

$$\frac{S}{N} = -10 * \log_{10}\left[\frac{1}{n}\left(\sum_{i=1}^{n} \frac{1}{{y_i}^2}\right)\right] \tag{3}$$

Target Value – Best

In this type of problem, a specific target value (such as product dimensions) is given:

$$\frac{S}{N} = \log\left(\sum_{i=1}^{n} \frac{y^2}{s^2}\right) \tag{4}$$

In all three cases, the goal is to maximize the S/N ratio.

In this study, the compressive, flexural, and impact strength values of hybrid fiber-reinforced concrete were analyzed based on the largest - best criterion. The signal-to-noise ratio (SN ratio) graphs resulting from these analyses are presented below.

Figure 9 shows the SN ratios for the 28-day compressive strength of concrete. It is observed that as the cement dosage and steel fiber content increase, the compressive strength also increases. Additionally, while there are fluctuations in the polypropylene and basalt fiber content, it is generally noted that an increase in these fibers leads to a decrease in compressive strength.

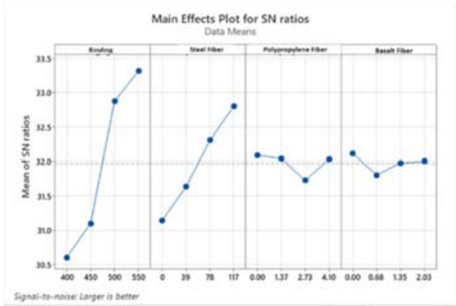

Model Summary

S	R-sq	R-sq(adj)	PRESS	R-sq(pred)	AICc	BIC
2.10561	92.08%	89.21%	102.295	83.40%	84.57	79.87

Analysis of Variance

Source	DF	Seq SS	Contribution	Adj SS	Adj MS	F-Value	P-Value
Regression	4	567.328	92.08%	567.328	141.832	31.99	0.000
Binding	1	419.485	68.09%	419.485	419.485	94.62	0.000
Steel Fiber	1	142.060	23.06%	142.060	142.060	32.04	0.000
Polypropylene Fiber	1	5.538	0.90%	5.538	5.538	1.25	0.288
Basalt fiber	1	0.246	0.04%	0.246	0.246	0.06	0.818
Error	11	48.769	7.92%	48.769	4.434		
Total	15	616.098	100.00%				

Figure 9 - SN ratio graphs for 28-day concrete compressive strength and Taguchi Analysis ANOVA Results

In order to assess the accuracy of the SN ratios for concrete compressive strength and identify the most influential parameter, an ANOVA (Analysis of Variance) was conducted. The ANOVA table is structured to generate a p-value, which facilitates the testing process by indicating the smallest level of significance at which the null hypothesis (H0) can be rejected. In the program output, a p-value of 0.05 is typically accepted. Hypotheses with values smaller than this are considered acceptable. Furthermore, the analysis table in Figure 9 shows which parameters contribute most significantly to compressive strength.

According to these results, the R-squared value of 92.08% indicates a high level of significance for the hypothesis. Furthermore, the ANOVA p-value being 0.0 supports this finding. Additionally, the binder contributes the most to concrete compressive strength at 68.09%, followed by steel fibers at 23%, and to a lesser extent, polypropylene and basalt fibers contribute slightly.

For flexural strengths, the SN ratio is presented in Figure 10. It shows that an increase in cement dosage and steel fiber content correlates with an increase in flexural strength. Additionally, an increase in polypropylene content partially increases flexural strength, while the effect of basalt fiber on flexural strength is limited. It is understood that macro polypropylene fibers contribute to a limited increase in flexural strength due to their potential for fracture in bending, whereas micro basalt fibers do not significantly affect flexural strength. Moreover, it is anticipated that the strong effect of macro fibers on flexural strength limits the impact of basalt fibers.

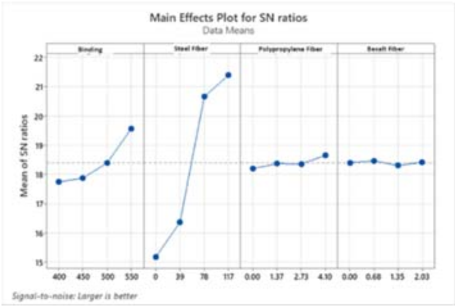

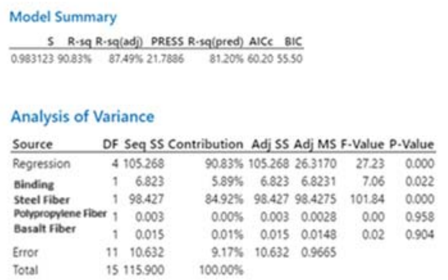

Model Summary

S	R-sq	R-sq(adj)	PRESS	R-sq(pred)	AICc	BIC
0.983123	90.83%	87.49%	21.7886	81.20%	60.20	55.50

Analysis of Variance

Source	DF	Seq SS	Contribution	Adj SS	Adj MS	F-Value	P-Value
Regression	4	105.268	90.83%	105.268	26.3170	27.23	0.000
Binding	1	6.823	5.89%	6.823	6.8231	7.06	0.022
Steel Fiber	1	98.427	84.92%	98.427	98.4275	101.84	0.000
Polypropylene Fiber	1	0.003	0.00%	0.003	0.0028	0.00	0.958
Basalt Fiber	1	0.015	0.01%	0.015	0.0148	0.02	0.904
Error	11	10.632	9.17%	10.632	0.9665		
Total	15	115.900	100.00%				

Figure 10 - SN ratio graphs for 28-day concrete flexural strength and Taguchi analysis bending test Anova results

According to the results in Figure 10, the R-squared value of 90.83% indicates a high level of significance for the hypothesis. Additionally, the ANOVA p-value being 0.0 supports this finding. Furthermore, steel fibers contribute the most to flexural strength at 94.92%, followed by binder at 5.89%, and to a lesser extent, polypropylene and basalt fibers affect flexural strength.

The SN ratio for Energy Absorption Capacity is presented in Figure 11. It shows that an increase in binder and steel fiber content correlates with an increase in energy absorption capacity. Additionally, an increase in basalt fiber content at dosages of 0.68 and 1.35 shows an increase in energy absorption capacity. Moreover, an increase in polypropylene fiber contribution partially increases energy absorption capacity, while the effect of basalt fiber on energy absorption capacity is limited. Furthermore, it is observed that the contribution of steel fiber content to energy absorption capacity remains almost the same between 1% and 1.5% variations. This result is due to the calculations being based on a 5 mm deflection. It is anticipated that if the energy absorption capacity were calculated based on a 10 mm deflection, an increase would be more pronounced at a fiber content of 1.5%.

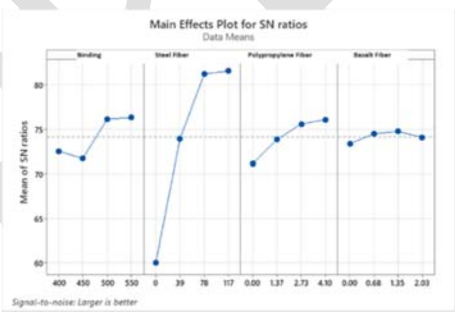

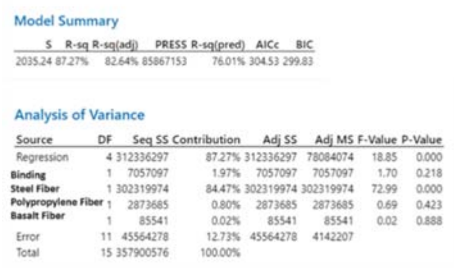

Model Summary

S	R-sq	R-sq(adj)	PRESS	R-sq(pred)	AICc	BIC
2035.24	87.27%	82.64%	85867153	76.01%	304.53	299.83

Analysis of Variance

Source	DF	Seq SS	Contribution	Adj SS	Adj MS	F-Value	P-Value
Regression	4	312336297	87.27%	312336297	78084074	18.85	0.000
Binding	1	7057097	1.97%	7057097	7057097	1.70	0.218
Steel Fiber	1	302319974	84.47%	302319974	302319974	72.99	0.000
Polypropylene Fiber	1	2873685	0.80%	2873685	2873685	0.69	0.423
Basalt Fiber	1	85541	0.02%	85541	85541	0.02	0.888
Error	11	45564278	12.73%	45564278	4142207		
Total	15	357900576	100.00%				

Figure 11 - Energy absorption capacity SN ratio graph and Anova results of Taguchi analysis for Energy Absorption Capacity (EAC) experiment.

The energy absorption capacity Anova results are given in Figure 11. According to these results, an R-squared value of 82.64% indicates that the hypothesis is statistically significant. Additionally, with an Anova p-value of 0.0, this supports the significance of the findings. Furthermore, steel fiber contributes the most, with 84.47% enhancement in energy absorption capacity. There is also a minor contribution from the binder. Polypropylene and basalt fiber additions contribute very little. Since energy absorption capacity largely depends on the increase in ductility of the material, steel fiber contributes significantly to this parameter. However, these results are not applicable to all concretes; they only reflect the mixtures studied in this research.

The Signal-to-Noise (S/N) ratio for the visible first crack impact count is presented in Figure 12. As observed, an increase in binder dosage, steel fiber content, and polypropylene fiber content leads to an increase in the number of visible first cracks. Additionally, it is noted that the influence of basalt fiber content on the first crack impact count is limited. The contribution of polypropylene macro fibers is observed when a dosage of 4.10 kg/m³ is used. This is attributed to the low content of fibers and their lesser impact compared to steel fibers.

Furthermore, while the contribution of microfibers to the first crack impact count was expected, the impact of basalt fibers in the process from elastic to plastic behaviour was not observed.

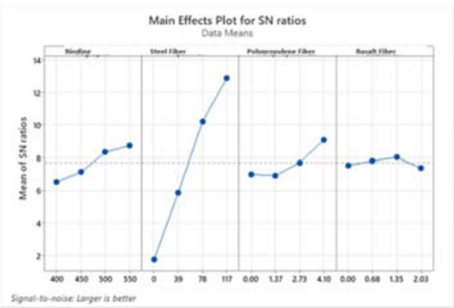

Model Summary

S	R-sq	R-sq(adj)	PRESS	R-sq(pred)	AICc	BIC
0.311652	95.75%	94.20%	2.68084	89.33%	23.44	18.74

Analysis of Variance

Source	DF	Seq SS	Contribution	Adj SS	Adj MS	F-Value	P-Value
Regression	4	24.0670	95.75%	24.0670	6.0167	61.95	0.000
Binding	1	0.7322	2.91%	0.7322	0.7322	7.54	0.019
Steel Fiber	1	23.0838	91.84%	23.0838	23.0838	237.67	0.000
Polypropylene Fiber	1	0.2377	0.95%	0.2377	0.2377	2.45	0.146
Basalt Fiber	1	0.0133	0.05%	0.0133	0.0133	0.14	0.719
Error	11	1.0684	4.25%	1.0684	0.0971		
Total	15	25.1354	100.00%				

Figure 12 - Results of first crack impact count shown as S/N ratios grap and Anova results for the first crack impact count

Figure 12 presents the Anova results for the first crack impact count. According to these results, an R-squared value of 95.75% indicates a high level of significance for the hypothesis. Additionally, with an Anova p-value of 0.0, this supports the significance of the findings. Furthermore, steel fiber contributes the most to the first crack impact count, with 91.84% enhancement. There is also a minor contribution from the binder. Polypropylene and basalt fiber additions contribute very little. It is observed that parameters contributing to tensile strength mostly influence the first crack impact count.

The Signal-to-Noise (S/N) ratio for the fracture impact count (at 100 mm deflection) is presented in Figure 13. It is observed that as binder dosage, steel fiber content, and polypropylene fiber content increase, the fracture impact count also increases. Additionally, the influence of basalt fiber content on the fracture impact count is seen to be limited. The contribution of polypropylene macro fibers is observed when a dosage of 4.10 kg/m³ is used. This is attributed to the lower content of fibers and their lesser impact compared to steel fibers.

Furthermore, the contribution of macro fibers to the fracture impact count is consistent with literature, indicating their expected role. The interlocking and pullout processes of macro steel fibers have influenced the fracture impact counts.

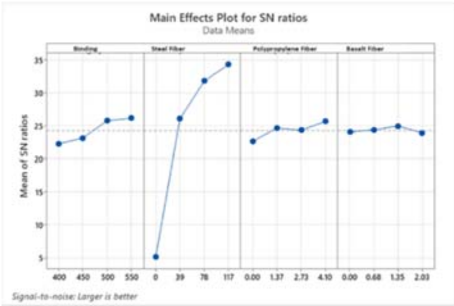

Model Summary

S	R-sq	R-sq(adj)	PRESS	R-sq(pred)	AICc	BIC
6.04768	93.83%	91.59%	794.176	87.82%	118.33	113.64

Analysis of Variance

Source	DF	Seq SS	Contribution	Adj SS	Adj MS	F-Value	P-Value
Regression	4	6119.00	93.83%	6119.00	1529.75	41.83	0.000
Binding	1	227.32	3.49%	227.32	227.32	6.22	0.030
Steel Fiber	1	5839.65	89.55%	5839.65	5839.65	159.66	0.000
Polypropylene Fiber	1	8.71	0.13%	8.71	8.71	0.24	0.635
Basalt Fiber	1	43.32	0.66%	43.32	43.32	1.18	0.300
Error	11	402.32	6.17%	402.32	36.57		
Total	15	6521.32	100.00%				

Figure 13 - Fracture impact count results shown as S/N ratios graph and Fracture Impact Count Anova Results

Figure 13 presents the Anova results for the fracture impact count. According to these results, an R-squared value of 91.59% indicates a high level of significance for the hypothesis. Additionally, with an Anova p-value of 0.0, this supports the significance of the findings. Furthermore, steel fiber contributes the most to the fracture impact count, with 89.55% enhancement. There is also a minor contribution from the binder. Polypropylene and basalt fiber additions contribute very little. It is observed that parameters contributing to tensile strength mostly influence the fracture impact count.

Table 12 presents the decibel (dB) values for the variables tested in their maximum amounts, including compressive strength, flexural strength, energy absorption capacity (EAC), first crack impact strength, and fracture impact strength. These values provide insight into the influence of the selected variables on the mechanical properties of mixed fiber concrete.

According to the data in Table 12, each component exhibits different performances in various mechanical properties. Binder generally shows the highest performance; it provides the highest value in compressive strength with 33.32 dB and also stands out with 19.56 dB in flexural strength. ÇL, on the other hand, shows the highest value in energy absorption capacity (81.52 dB) and also excels in flexural strength with 21.39 dB. PPL generally performs well, achieving a strong value of 32.03 dB in compressive strength, but it falls short compared to ÇL in flexural strength with 18.65 dB. In terms of energy absorption capacity, it provides a value of 76.04 dB, which is close to Binder's performance. BL, compared to the other components, generally has lower values, particularly in compressive strength, where it lags behind with 32.00 dB. However, BL still demonstrates sufficient performance in certain properties, particularly in energy absorption capacity, where it shows the lowest value of 74.06 dB. These results indicate that each component contributes to different mechanical properties of concrete, and while PPL shows strong performance in certain areas, ÇL outperforms in some properties.

Table 12 - Determining the Taguchi Optimum Concrete Mix and Experimental Results

	Decibel values of variables used in maximum amounts				
Series	Reference Line	Binder	ÇL	PPL	BL
Compressive Strength	31.97	33.32	32.80	32.03	32.00
Flexural Strength	18.39	19.56	21.39	18.65	18.41
EAC	74.14	76.29	81.52	76.04	74.06
First Crack Impact Strength	7.67	8.73	12.87	9.08	7.35
Fracture Impact Strength	24.27	26.09	34.25	25.62	23.85

3.1. Taguchi Optimization of Experimental Results

The optimization results obtained by analyzing the highest-best Taguchi S/N ratios are presented in Table 13. For compressive strength, the mixture with a binder ratio of 550 kg/m³ and steel fiber of 117 kg/m³ yields the highest result. For flexural and first crack impact strength, the optimal mixture includes a binder ratio of 550 kg/m³, steel fiber of 117 kg/m³, and polypropylene fiber at 4.10 kg/m³. Additionally, for fracture impact strength and toughness, the highest results are achieved with a binder ratio of 550 kg/m³, steel fiber of 117 kg/m³, polypropylene fiber at 4.10 kg/m³, and basalt fiber at 1.34 kg/m³.

Table 13 - Determining the Taguchi Optimum Concrete Mix and Experimental Results

Properties	**Binding (kg/m^3)**	**SF (kg/m^3)**	**PF (kg/m^3)**	**BF (kg/m^3)**	**Matched Series (kg/m^3)**
28 Day Pressure	550	117	0	0	No (The nearest is K16)
Bending	550	117	4.10	0	No
First crack Impact	550	117	4.10	0	No
Fracture Impact	550	117	4.10	1.35	No
Satiety	500-550	78-117	4.10	1.35	No
OP1	550	117	4.10	0	Bending, İmpact, Satiety
OP2	550	117	0	0	Pressure Strenght

According to the evaluations in Table 12, experimental series OP1 is identified as optimal for Flexural Strength, Toughness, and Impact Strength, while experimental series OP2 is determined as optimal for Compressive Strength. This determination was based on the highest-best assessment. Prediction analyses and verification experiments were conducted to validate the accuracy of these series and the Taguchi mathematical model.

3.2. Taguchi Validation Experiments

The Taguchi optimization experiments for series OP1 and OP2, designated for Compressive, Flexural, and Impact Strength tests, were conducted. The results of Taguchi prediction analyses and experimental data are presented in Table 14. The proximity between the optimization experiment results and the predicted outcomes demonstrates the success of this method.

Table 14 - Optimization Prediction Data and Experimental Results

Series	Pressure (28 days, MPa)	Pressure (90 days, MPa)	Flexural Strength (MPa)	Impact Initial (number of blows)	Impact Final (number of blows)	Toughness (N.mm)
OP1(Predict)	51.07	57.56	13.01	4.98	61.89	14495.3
OP1(Experiment)	54.14	58.99	13.97	5.66	65.67	13707.2
OP2(Predict)	52.191	59.76	12.94	4.64	61.88	13196.5
OP2(Experiment)	60.44	64.21	12.36	5	56.33	11137.3

Figure 14 - Experimental results for optimization and Taguchi series

When comparing Taguchi prediction and experimental results, the error of the mathematical model according to regression results does not exceed 15%. This standard deviation is already within the error margin of the experimental data, confirming the validation of the mathematical model.

All experimental results for both control and optimization series are presented in Figure 14. The comparison of optimization series is visually identified in the graph.

4. DISCUSSION

In the experimental studies and Taguchi analyses conducted, it was observed that concrete compressive strength increases with the addition of fiber reinforcement. Tawfiq, Jamshid, and Rodolfo [22] explained this phenomenon by noting that monofilament fibers have a high Young's modulus, which makes them more resistant to compressive loads. They also mentioned that monofilament fibers spread within concrete, easily forming a network between cracks and reducing stress concentrations along crack lines.

Taguchi analyses indicated that binder dosage primarily influences concrete compressive strength, with additional contributions from the inclusion of fibers. It was found that polypropylene and basalt fibers lead to a decrease in concrete compressive strength due to the formation of voids within the matrix.

A recent study by Johnson [23] confirms that the incorporation of fibers, particularly steel fibers, significantly improves the compressive and flexural strengths of concrete. Similar to the findings in the paper, the study emphasizes the importance of fiber-matrix bonding and optimal fiber volume ratios for achieving maximum performance.

Another publication by Lee et al. [24] discusses the role of hybrid fibers in concrete. The combination of different fiber types (e.g., steel and polypropylene) can mitigate the drawbacks of using a single fiber type. This hybrid approach aligns with the observation that using polypropylene or basalt fibers alone does not significantly enhance flexural strength.

In this study, the addition of fibers consistently increased the compressive, flexural and other mechanical properties, and optimum improvement was observed when the fiber volume remained below 2%. In a study by Yoa et al. [25], it was shown that the maximum increase in flexural strength in fiber-reinforced concrete occurred at a fiber volume ratio of 3%. Beyond this point (at 4% fiber content), flexural performance began to decrease, with the composite material containing 4% fiber volume showing the lowest compressive performance among the tested mixtures. Recent research by Zhang et al. [26] corroborates the optimal fiber volume ratio findings. Their study indicates that beyond a certain fiber content (around 3-4%), the mechanical properties of fiber-reinforced concrete begin to decline due to fiber agglomeration and void formation. This matches the results mentioned in the paper, where a 4% fiber volume ratio showed decreased flexural performance.

In this study, the contribution of steel fibers with higher modulus of elasticity to the performance was higher than PPF and BF. This was highlighted by Kumar et al. [27], who highlighted the importance of fiber length and type on the performance of fiber reinforced concrete. The study found that longer fibers with higher tensile strength contributed to better post-crack behavior and overall mechanical properties, reflecting the observations in the paper on tensile strength and fracture behavior of longer fibers.

The pullout and breakage of fibers, dependent on fiber-matrix interface properties and fiber length, tend to enhance post-crack fracture mechanisms in fiber-reinforced concrete under tensile loading. Longer fibers, which better bond with the cement matrix, tend to exhibit higher pullout forces and can break without complete detachment. In experimental studies, when PPF was used together with SF, it exhibited pull-out behavior. This indicates that the use of PPF together with SF is more effective in enhancing performance. Additionally, it was observed that SF should be used at a minimum of 1% of the concrete volume; otherwise, it tends to pull out rather than rupture.

In this study, it was observed that an increase in fiber content reduced the percentage of breakage in steel fiber-reinforced concrete. This reduction was attributed to decreased stress on the fibers as their number increased. The impact ratio of steel fibers, binder, polypropylene, and basalt fiber additions sequentially enhanced flexural strength. However, it was found that using polypropylene or basalt fibers alone did not significantly increase flexural strength. In the study by Yoa et al. [28], it was determined that the addition of fibers increased the modulus of rupture across all fiber types. Among the three types of fibers, steel fibers provided the highest modulus of rupture, while polypropylene fibers yielded the lowest. Steel-PP fiber concrete slightly increased the modulus of rupture compared to concrete with only PP fibers but reduced strength compared to simple steel fibers.

This study also observed that steel fibers primarily enhanced concrete ductility and post-crack behavior. The contribution of polypropylene fibers, as indicated by Taguchi analyses, was observed to be less than 1%. Contributions from basalt fibers to flexural and impact strength were not observed, likely due to the microfiber nature of basalt fibers and the lower tensile strength of polypropylene fibers compared to steel. Regarding impact strength of fiber-reinforced concretes, it was found that steel fibers contributed most to impact resistance until the first crack appeared, after which concrete strength played a larger role. Contributions from polypropylene and basalt fibers were limited. Beyond the first crack, up to a deflection of 10 cm, impact resistance was primarily influenced by the pulling and breaking behavior of steel fibers. The findings of this study align with previous research emphasizing the superior performance of steel fibers in enhancing the impact resistance of concrete. Yazıcı et al. [4] demonstrated that the maximum particle size of aggregate should not exceed 20 mm for optimal impact resistance, corroborating the importance of aggregate selection in this study. Kızılırmak et al. [5] found that reducing the water-cement ratio improves concrete strength, which supports the approach taken in this research to maintain a low water-cement ratio. Nili and Afroughsabet [7] highlighted the benefits of silica fume in improving fiber distribution and mechanical properties in fiber-reinforced concrete. This study's use of silica fume as a mineral additive aligns with their findings, showing enhanced strength and durability in the concrete mixes.

Overall, within the scope of this study, it was determined that the use of steel fibers and binder dosage most significantly influenced flexural, toughness, and impact strength parameters in concrete. The addition of polypropylene fibers did not contribute significantly to the mechanical properties of concrete, likely due to the restraining effect of high-strength, hooked steel fibers. Additionally, it was observed that binder dosage effectively influenced concrete compressive strength, aligning with findings in the literature. The findings in the paper are consistent with recent research trends and publications in the field of fiber-reinforced concrete. The importance of optimal fiber volume ratios, fiber-matrix interface properties, and the type and length of fibers are well-supported by current literature.

5. CONCLUSION AND RECOMMENDATION

In this study, the effects of binder content, and steel, polypropylene, and basalt fiber amounts on the compressive, flexural, and impact strength of fiber-reinforced concrete were investigated. In this context, an L16 (4^4) matrix was created using Taguchi optimization technique, leading to the formulation of 16 concrete series for experimental investigations. Subsequently, optimization analysis and validation experiments were conducted. Taguchi analyses were validated, and the optimization and analyses were accepted.

i. Tensile Strength and First Crack Impact Number: The highest results for tensile strength and the number of first crack impacts were obtained with a binder ratio of 550 kg/m³, steel fiber 117 kg/m³, and polypropylene fiber 4.10 kg/m³. These findings are consistent with existing studies in the literature and demonstrate that the fiber-matrix bond plays a significant role in enhancing concrete performance. The high binder content creates a dense, cohesive matrix that ensures strong fiber anchorage and effective stress transfer. Steel fibers, with their high modulus of elasticity, act as primary reinforcement by bridging cracks and dissipating energy, while polypropylene fibers control micro-cracks and improve cohesiveness, reducing segregation and enhancing the distribution of steel fibers. This hybrid fiber system leverages the complementary properties of steel and polypropylene fibers, with steel fibers resisting macro-cracks and polypropylene fibers preventing shrinkage cracks, ultimately leading to superior tensile strength and impact resistance. The strong fiber-matrix bond, coupled with the dense matrix, delays crack initiation and propagation, highlighting the importance of fiber-matrix interaction in optimizing concrete performance.

ii. Number of Fracture Impacts and Durability: The highest number of fracture impacts and durability results were obtained using a binder ratio of 550 kg/m³, steel fiber 117 kg/m³, polypropylene fiber 4.10 kg/m³, and basalt fiber 1.34 kg/m³. This shows that combining different types of fibers is effective in optimizing the mechanical properties of concrete. The highest fracture impacts and durability results were achieved due to the synergistic effects of the optimal combination of binder ratio and fibers. A binder ratio of 550 kg/m³ ensures a dense and durable concrete matrix, enhancing hydration and strength. The addition of 117 kg/m³ steel fibers improves tensile strength, fracture toughness, and resistance to cracking by distributing stresses more evenly and reducing crack propagation. Polypropylene fibers at 4.10 kg/m³ control plastic shrinkage cracking and improve impact resistance, especially during early curing stages. Basalt fibers, at 1.34 kg/m³, enhance durability by providing resistance to corrosion, chemical attack, and environmental degradation, while also improving fracture toughness. Together, these fibers create a concrete that offers superior fracture resistance, impact absorption, and long-term durability, making it highly effective in withstanding both mechanical stresses and harsh environmental conditions.

iii. Compressive Strength of Concrete: The study observed that fiber reinforcement increases the compressive strength of concrete. Steel fiber content, binder, and silica fume ratios were identified as the factors with the most significant effects on the impact resistance of concrete. As the binder content increases, the amount of hydration products also increases, which enhances the strength. It has been observed that the compressive strength of concrete is higher with the addition of steel fibers. This phenomenon has been explained by the fact that monofilament fibers have a high elasticity modulus, making them more resistant to compressive loads. The spread of monofilament fibers within the concrete helps easily form a network between cracks, reducing stress concentration at crack lines. Polypropylene fibers, having a lower elasticity modulus, undergo significant deformation under compression. However, due to their lower elasticity modulus, they behave as small voids in the concrete, which leads to a reduction in compressive strength.

It was determined that steel fibers contribute 23% to the compressive strength of fiber-reinforced concrete, while the binder content accounts for 68%. Additionally, it was found that the effect of polypropylene and basalt fibers is limited but adversely affects compressive strength.

Observations revealed that the toughness, flexural, and impact strength of fiber-reinforced concrete are influenced by the tensile strength of the concrete, with fiber additives contributing positively to these properties. It was further observed that steel fibers contribute most significantly to these properties. However, the impact of basalt fibers was found to be minimal.

Taguchi optimization experiments confirmed that this method can be applied not only within the same material group but also across different types of materials. It was demonstrated that Taguchi analyses provide accurate results for parameters affecting various concrete properties.

The recommendations in the study include general observations but could benefit from specific, actionable suggestions to guide further investigations. Based on the provided content, here are refined recommendations that align with the study's findings and could be investigated further:

Fiber Synergy and Optimization: Explore the effects of varying proportions of steel, polypropylene, and basalt fibers in hybrid combinations, focusing on their contributions to specific mechanical properties like impact resistance and flexural strength. Investigate whether alternate combinations could outperform the optimal mix identified in this study.

Matrix-Fiber Bond Enhancement: Examine methods to improve the fiber-matrix bond, such as using surface-treated or coated fibers, to enhance mechanical performance and reduce fiber pull-out.

Scaling and Practical Applications: Conduct large-scale tests to validate the laboratory findings under real-world conditions, including structural-scale specimens subjected to dynamic loads.

Environmental and Durability Aspects: Investigate the long-term durability of the optimized fiber-reinforced concrete under varying environmental conditions, such as freeze-thaw cycles, chemical exposure, and sustained loading.

Binder Content Variation: Analyze the effects of different binder types and supplementary cementitious materials (e.g., fly ash, slag) on the performance of fiber-reinforced concrete, focusing on sustainability and cost-effectiveness.

Impact of Fiber Length and Distribution: Study the influence of varying fiber lengths and distribution patterns on mechanical properties, especially for impact and flexural performance.

Advanced Analytical Techniques: Employ advanced imaging and analytical techniques, such as X-ray CT scanning, to study the internal distribution and orientation of fibers and their correlation with observed mechanical behavior. These targeted suggestions would not only build on the study's findings but also provide a clear roadmap for future research.

Acknowledgements

This research was conducted within the scope of the doctoral program in the thematic field of YÖK 100/2000 "building-building material-construction management", the SDÜ BAP project with project code FDK-2022-8439 and TUBITAK BİDEB 2211 programs. The authors would like to thank SDÜ BAP unit, YÖK and those who contributed to the YÖK 100/2000 program.

Reference

[1] Arıcı, E., Dursun, R., & İnce, R. (2007). Betonun Çarpma Mukavemetinin Tesbiti.

[2] Anık, S., Metalik Malzemelerin Mekanik Deneyleri, Birsen Yayın Evi, İstanbul, 1999.

[3] Oltulu, M., & Altun, M. G. (2018). Betonun Darbe Dayanımının Tespitinde Ağırlık Düşürme Deney Yöntemi Ve Yapılan Çalışmalar. Gümüşhane Üniversitesi Fen Bilimleri Enstitüsü Dergisi, 8(1), 155-163.

[4] Yazıcı, Ş., & Sezer, G. İ. (2008). Çelik Lifli Betonların Darbe Direncine Agrega Maksimum Boyutunun Etkisi. Pamukkale Üniversitesi Mühendislik Bilimleri Dergisi, 14(3), 237-245.

[5] Kızılırmak, C., Aydın, S., & Yardımcı, M. Y. (2019). Çelik Lif Kanca Geometrisinin Yüksek Dayanımlı Lifli Betonların Statik Ve Darbe Yükleri Altında Eğilme Özelliklerine Etkisi. Journal Of The Faculty Of Engineering & Architecture Of Gazi University, 34(3).

[6] Nataraja, M. C., Nagaraj, T. S., & Basavaraja, S. B. (2005). Reproportioning Of Steel Fibre Reinforced Concrete Mixes And Their İmpact Resistance. Cement And Concrete Research, 35(12), 2350-2359.

[7] Nili, M., & Afroughsabet, V. (2010). The effects of silica fume and polypropylene fibers on the impact resistance and mechanical properties of concrete. Construction and Building Materials, 24(6), 927-933.

[8] Mohammadi, Y., Carkon-Azad, R., Singh, S. P., & Kaushik, S. K. (2009). Impact resistance of steel fibrous concrete containing fibres of mixed aspect ratio. Construction and Building Materials, 23(1), 183-189.

[9] Yavaş, A., Birol, T., Türker, K., Hasgül, U., vd. (2020). Improvement on Flexural Performance of UHPFRC with Hybrid Steel Fiber. Teknik Dergi, 31(6), 10379-10397. https://doi.org/10.18400/tekderg.485

[10] Soufeiani, L., Raman, S. N., Jumaat, M. Z. B., Alengaram, U. J., Ghadyani, G., & Mendis, P. (2016). Influences Of The Volume Fraction And Shape Of Steel Fibers On Fiber- Reinforced Concrete Subjected To Dynamic Loading–A Review. Engineering Structures, 124, 405-417.

[11] Banthia, N., Yan, C., & Sakai, K. (1998). Impact Resistance Of Fiber Reinforced Concrete At Subnorma Temperatures. Cement And Concrete Composites, 20(5), 393-404.

[12] Türker, K., Birol, T., Yavaş, A., Hasgül, U., vd. (2019). Ultra Yüksek Performanslı Lifli Beton İçeren Kirişlerin Eğilme Davranışı. Teknik Dergi, 30(1), 8777-8801. https://doi.org/10.18400/tekderg.287116.

[13] Sharifi, E., Sadjadi, S. J., Aliha, M. R. M., & Moniri, A. (2020). Optimization of high-strength self-consolidating concrete mix design using an improved Taguchi optimization method. Construction and Building Materials, 236, 117547.

[14] Tanyildizi, H., & Şahin, M. (2015). Application of Taguchi method for optimization of concrete strengthened with polymer after high temperature. Construction and Building materials, 79, 97-103.

[15] Mehta, A., Siddique, R., Singh, B. P., Aggoun, S., Łagód, G., & Barnat-Hunek, D. (2017). Influence of various parameters on strength and absorption properties of fly ash based geopolymer concrete designed by Taguchi method. Construction and Building Materials, 150, 817-824.

[16] Lei, B., Li, W., Liu, H., Tang, Z., & Tam, V. W. (2020). Synergistic effects of polypropylene and glass fiber on mechanical properties and durability of recycled aggregate concrete. International Journal of Concrete Structures and Materials, 14, 1-14.

[17] Mindess S., Young F.J., "Concrete", Prentice-Hall Inc., 1981, p.1, 6-7, 119-137, 184-185, 600, 603, 628-634.

[18] Donza H., Cabrera O., Irassar E.F., High-strength concrete with different fine aggregate, Cement and Concrete Research 32, 2002, p.1755-1761.

[19] Zhang, W., Chen, S., & Liu, Y. (2017). Effect of weight and drop height of hammer on the flexural impact performance of fiber-reinforced concrete. Construction and Building Materials, 140, 31-35.

[20] TS EN 206-1 "Beton-Bölüm 1: Özellik, Performans, İmalat ve Uygunluk", Turk Standardları Enstitüsü, 2002.

[21] Şirvancı, M. (1997). Kalite için deney tasarımı" Taguçi yaklaşımı". Literatür.

[22] Tawfiq, K., Amaghani, J., & Ruiz, R. (1999). Fatigue cracking of polypropylene fiber reinforced concrete. Materials Journal, 96(2), 226-233.

[23] Janson, A. (2023). Influence of Fiber Properties on the Behavior of Fiber-Reinforced Concrete (Master's thesis, University of Minnesota).

[24] Lee, H., Choi, M. K., & Kim, B. J. (2023). Structural and functional properties of fiber reinforced concrete composites for construction applications. Journal of Industrial and Engineering Chemistry, 125, 38-49.

[25] Yao, W., Li, J. ve Wu, K. (2003). Mechanical properties of hybrid fiber reinforced concrete at low fiber volume fraction. Cement and concrete research, 33 (1), 27-30.

[26] Zhang, D. M., Zhou, W. D., Bu, X. H., Jiang, Y., Jia, K., & Yang, G. H. (2022). Failure mechanism and stiffness degradation of double lining with inner R/FRC lining subjected to internal water pressure. Tunnelling and Underground Space Technology, 130, 104737.

[27] Kumar, R., Babu, T. R., Venkatesan, G., Padhi, S. N., Parida, J. L., & Kumar, V. R. (2023). Investigation of fiber reinforced concrete–Energy absorption capacity with steel and polymeric fibers. Materials Today: Proceedings.

[28] Zollo, R. F. (1997). Fiber-reinforced concrete: an overview after 30 years of development. Cement and concrete composites, 19(2), 107-122.

[29] Balaguru, P. N., & Shah, S. P. (1992). Fiber-reinforced cement composites.